EFFECT OF CIRCULAR UNREINFORCED HOLES ON THE STABILITY OF AXIALLY LOADED CYLINDRICAL SHELLS IN THE ELASTICOPLASTIC ZONE

A. P. Shapovalov

UDC 624.074.001.24+539

Cylindrical shells are widely used in various industrial fields. Very often one or more holes, mostly of circular shape, are cut in them for structural or technological reasons. This leads to a reduction in the bearing capacity of the component as a whole or to a significant rearrangement of the pattern of the stressed—deformed state, in comparison with the unperforated case. In this connection the stability design of shells weakened by holes represents an important phase in the design of the whole component.

The stability of unperforated shells has already been studied fairly fully. On the other hand, the stability of a cylindrical shell weakened by circular holes presents a very complex theoretical problem which, notwithstanding its great practical value, has not been solved analytically up to the present time. Altogether, 12 publications [1] have been devoted to the stability of perforated shells, yet all of these excepting [2] were investigated by formulating the problem on an elastic base. As regards problems of the stability of perforated shells in the elasticoplastic zone, the analytical and computational difficulties involved in their solution are substantially increased and, in this connection, there are to our knowledge no theoretical solutions in this field. Nevertheless, perforated cylindrical shells, which are widely used in structures (e. g. aviation gas-turbine engines), lose their stability in the elasticoplastic zone, and therefore the investigation of the stability of such shells is of undoubted practical interest.

The search for means of solving the subject problem in the elasticoplastic zone will evidently have to be based on experimental investigations. The latter would make it possible to collect statistical data for the values of the critical forces, and also to study the qualitative nature of the cause of loss of stability; without a clear picture of the latter, a successful theoretical solution of the subject problem is very unlikely.

It should be noted that [2] describes the results of an investigation of 300 shell specimens with constant geometric parameters R_{av}, δ, and L.

The present article brings forward the results of investigations conducted on specimens of different geometric parameters R_{av}, δ, and L. This made it possible to examine the qualitative nature of stability loss more fully and in greater depth. Simultaneously, more definite determinations were made of the limits of the effects of perforations on stability, depending on their location on the shell surfaces and on the geometric parameters of the shells. The data obtained can be used for shells having a wide range of changes in their characteristics.

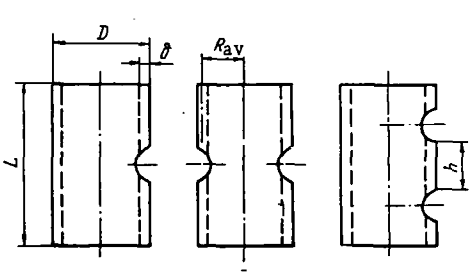

Fig. 1. Schematic diagrams of locations of weakening perforations.

Several series of tests were made, aimed at determining the effect of circular holes on the stability of cylindrical shells subjected to axial loading. Altogether 966 shells were tested, the number and radii of the holes being varied, also their distribution over the surface, and the shell lengths. The nature of such weakening of the shells tested, together with indications of the geometric parameters used in analyzing the test results, are shown in Fig. 1.

Zaporozh'e Branch of the Dnepropetrovsk Metallurgical Institute. Translated from Problemy Prochnosti, No. 5, pp. 113-118, May, 1974. Original article submitted October 18, 1972.

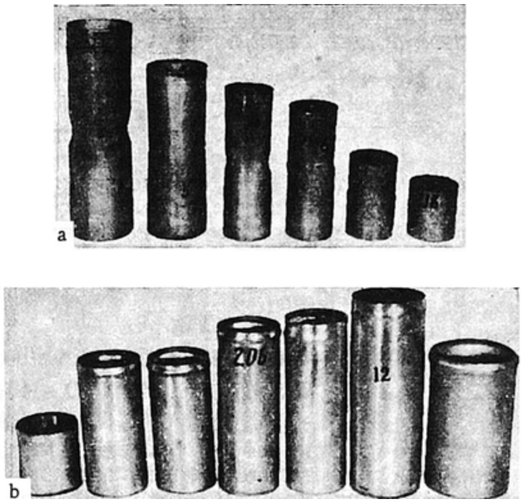

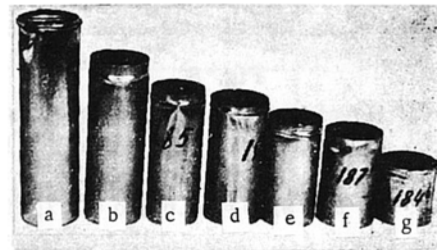

Fig. 2

Fig. 3

Fig. 2. Forms of stability loss of shells which are (a) weakened by holes and (b) unperforated.

Fig. 3. Formation of crinkles upon loss of stability of shells with $R_{av}/\delta \geq 60$.

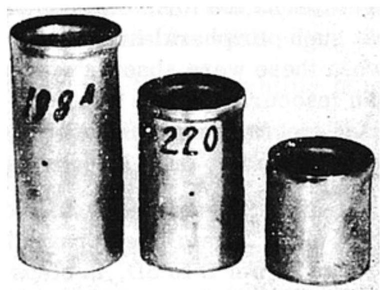

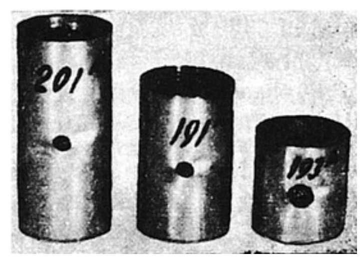

Fig. 4

Fig. 5

Fig. 4. Form of stability loss of shells with small holes.

Fig. 5. Effect of shell length on development of crinkle at hole.

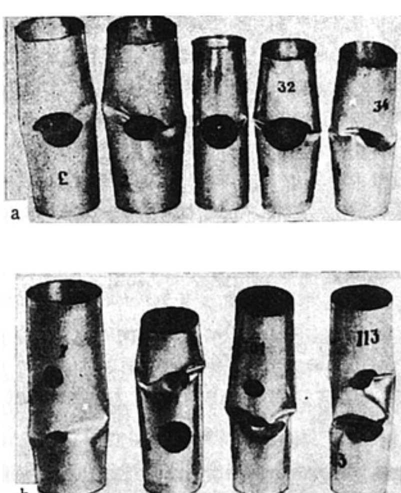

Fig. 6. Forms of complete loss of stability.

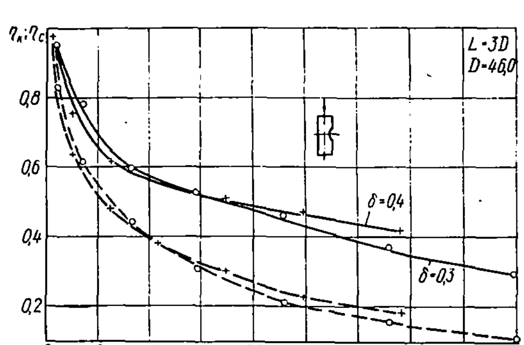

Fig. 7. Variation of critical load with weakening parameter ω.

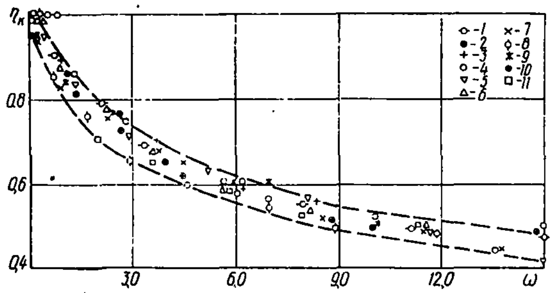

Fig. 8

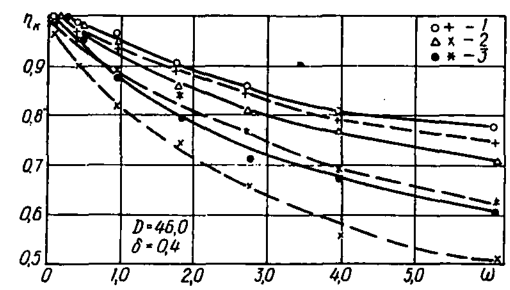

Fig. 9

Fig. 8. Envelope of scatter of experimental η_k values for shells with different values of D and δ (all dimensions are in mm): 1) D = 42, δ = 0.25; 2) D = 42, δ = 0.3; 3) D = 46, δ = 0.3; 4) D = 46, δ = 0.4; 5) D = 52.6, δ = 0.75; 6) D = 57, δ = 1.0; 7) D = 59.8, δ = 0.9; 8) D = 60, δ = 1.2; 9) D = 62.65, δ = 0.7; 10) D = 65, δ = 0.7; 11) D = 72, δ = 0.8.

Fig. 9. Variation of parameter η_k with type of weakening and shell length (full lines indicate shells with single midheight holes on one side, dashed lines indicate shells with through holes in the same position): 1) L = D; 2) L = 2D; 3) L = 3D.

In fabricating the specimens, strict attention was paid to ensure that the end faces would be parallel and also normal to the generatrices, thus providing uniform distribution of the axial force on the shell ends. In forming the holes, measures were taken to preserve the initial shape of the shell in the region of the hole, and no engineering imperfections were permitted in the form of tears, indents or creases of their periphery. It was experimentally established that such peripheral imperfections caused a scatter of critical-load values of up to 50%, as against only 8% when these were absent, within the limits of each specimen series tested. In addition it was noted that an inaccuracy in the hole cut, i. e. its departure from a strictly concentric shape, amounting in individual specimens up to 30% of the radius of the weakening hole, had practically no effect on the critical loads, provided no such inaccuracies were present.

The specimens were made of seamless pipes of heat-resisting steel, fabricated to close tolerances. Altogether 11 types of tube with dimensions ranging from 42 to 72 mm in external diameter and 0.25 to 1.2 mm in wall thickness were used. Tube lengths L ranged from D to 3D, in steps of 0.5D.

The mechanical properties of the tube material were determined directly from tube specimens, for which a special device was developed [3]. They were as follows: $\sigma_{pl} = 3 \cdot 10^8$ N/m², $\sigma_t = 3.5 \cdot 10^8$ N/m², $E = 2 \cdot 10^{11}$ N/m², and $\mu = 0.3$.

The shells were experimentally investigated within a wide range of characteristics [4]:

$$\frac{R_{av}}{\delta} = 28 - 83 \ll \frac{1}{\sqrt{3(1-\mu^2)}} \cdot \frac{E}{\sigma_{pl}} \approx 400.$$

A special universal stand was manufactured for conducting the tests, permitting both simple and complex loading, with a screw press for axial loading. Use was also made of a type GRM-1 machine with a special device [2]. The shells under test were placed in slotted holders which ensured a rigid clamping of the supported sections and a hinged transfer of forces onto the supporting disks. Illustrated in Fig. 2 are unperforated shells and shells weakened by through holes. The axially symmetrical form of the stability loss demonstrates the observance of end conditions and axial transmittal of the compressive forces.

A qualitative analysis of the forms of stability loss showed that they depend on two factors: the shell characteristic ratio R_{av}/δ and the weakening-hole radius.

The stability loss of unperforated shells with $R_{av}/\delta < 60$ is accompanied by the appearance of a symmetrical ring corrugation (see Fig. 2b) located close to one of the bearing faces. Not one of the numerous specimens manifested a ring corrugation in the mid-height zone of the shell, if it was not clamped at the ends.

Measurements of radial displacements along the shell generatrices showed that displacements increased more rapidly at their edges (bearing faces) than in the middle zone. Thus, distortion of the generatrices at the edges outstrips load increments. It is quite evident that even under axial compression there can be no moment-free condition in the material adjoining the shell ends, already in its pre-critical state.

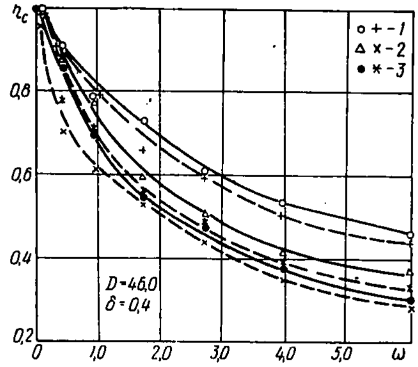

Fig. 10

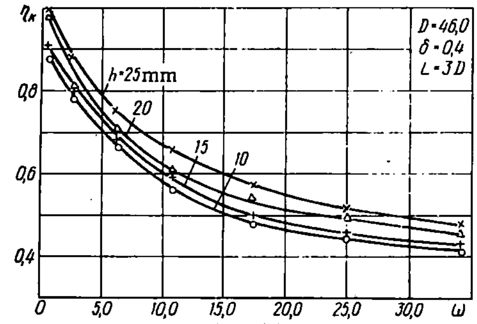

Fig. 11

Fig. 10. Variation of parameter η_c with type of weakening and shell length (for designations, see Fig. 9).

Fig. 11. Variation of parameter η_k with bridge height h between holes.

It was experimentally established that the region of distribution of the nonhomogeneous zone depends on the section shape of, and the technique used in fabricating, the end clamping ring. For shell lengths of $L \leq 3D$ and a rigid clamping device which is fabricated together with the shell and transitioned smoothly to the shell wall, the ring corrugations appearing in those cases where stability loss occurs are manifested in a zone located a distance of 0.75D to D from the shell edge. As the rigidity of the ring-applied end loading is diminished, and also with a more abrupt transition from the shell wall to the ring, the manifestation of the ring corrugation approaches the shell edge.

For shells with $R_{av} \geq 60$, loss of stability is manifested in the following forms:

(a) The ring corrugation and symmetrical longitudinal crinkles occur simultaneously (Fig. 3c and d).

(b) Ring corrugations and unsymmetrical longitudinal crinkles are formed simultaneously over the whole or part of the periphery (Fig. 3a, b, e, g).

(c) Longitudinal dents of rhombic shape are formed in zones close to the bearing faces (Fig. 3f).

For this shell type the form of stability loss is affected to some extent by their height.

The form of stability loss of shells which are weakened by small holes is the same as for unperforated specimens (Fig. 4).

With an increase in the size of the weakening holes, the loss of stability assumes a local character, and is accompanied by the appearance of plastic crinkles at the hole edge in zones of maximum disturbance of compressive stresses (Fig. 5). This very clearly demonstrates the effect of shell length on the dimension (length) of the crinkle.

For all specimens having the same values of parameters D and δ (see Fig. 5), the axial load was brought up to an identical value. However, measurements showed that in specimen 201A, which had a weakening hole of the same radius as that in specimen 191A, the crinkle length exceeded 2D, whereas in specimen 191A it was slightly over D. This is well detected by light-spot projection and also by specimen 193A in which the radius of the weakening hole is greater than in specimens 201A and 191A, yet the crinkle length is slightly less than D.

The specimens shown in Fig. 5 were not brought to a complete loss of bearing capacity; this occurred after the appearance of a crinkle.

The perforated shells can be divided into three groups according to the instants corresponding to the appearance of a plastic crinkle and complete loss of bearing capacity: The first includes shells with small holes, which lose general stability without manifesting crinkles in the region of the hole. The shells in the second group are characterized by the simultaneous loss of general stability and the appearance of a crinkle near the hole. The third comprises shells which exhibit plastic crinkles ahead of the general loss of bearing capacity; characteristically, as the hole radius is increased so does the difference between the load at which the plastic crinkle appears and the load causing complete loss of bearing capacity.

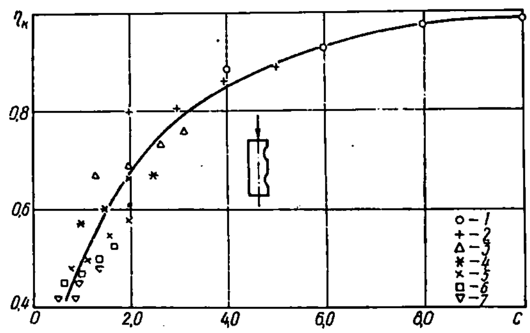

Fig. 12. Variation of η_k with weakening parameter: 1) $\omega = 0.69$; 2) $\omega = 2.76$; 3) $\omega = 6.23$; 4) $\omega = 11.05$; 5) $\omega = 17.3$; 6) $\omega = 24.6$; 7) $\omega = 34.0$.

Measurement of displacements in the region of the hole showed that the rate of change of shell surface shape is greater here than at any other part of the shell. Therefore, a moment-free state in this region does not occur right from the initial instant of loading. The loss of stability of shells in the third group is local in nature. Shells which were brought to a complete loss of bearing capacity are shown in Fig. 6.

The postulation, and lines of attack for the theoretical solution, of problems of the elastic stability of perforated plates and shells were developed by A. N. Guz' [5]. According to his classification, all stability problems are divided into three groups: 1) shells with small holes whose effects can be ignored; 2) shells with holes which affect critical loads; and 3) stability of perforated shells subjected to tensile loading.

Experimental investigations of stability under compressive loading fully confirmed the legitimacy of this classification for elasticoplastic shells also. The latter can likewise be subdivided into two groups: those with small holes having no effect on stability, and those with large holes affecting critical loadings.

For quantifying the test results, three values of the critical loads were used:

P_c is the lower value, corresponding to the commencement of the appearance of a plastic crinkle in the region of maximum disturbance of compressive stresses. In the first specimens this instant was determined by resistance strain gages. On all other specimens tested, the radial displacements in this region were measured with indicators having scale divisions of 1, 2, and 10 μ. The instant of initiation of a plastic crinkle was detected by the abrupt increase in the rotation rate of the indicator pointer, with the load increasing at a constant rate, this rotation hitherto being proportional to the load. At the instant of greater pointer rotation, the load stopped increasing. Simultaneously, the commencement of crinkle formation in all specimens was determined by projecting a ray onto a light spot. Correlation of the results obtained by the three methods showed a divergence of less than 3%.

P_k is the upper value, corresponding to the commencement of plastic deformation throughout the whole weakened section. This value was determined from the dynamometer scale of the testing machine or set-up, at the moment the dynamometer pointer stopped and all shell displacements increased rapidly. This instant is also easily discernible visually.

P_0 is the upper value of the experimentally determined critical load for unperforated shells (no weakening).

To ensure reliability of the experimental data, all three values of the critical load were determined from at least three specimens with identical geometric parameters D, L, δ, and ρ, where ρ is the radius of the weakening hole. The scatter of P_k values for the three specimens of a given series varied within the range 3 to 6%; for P_0 it was, respectively, 3 to 8% and 3 to 4%; which reflects the accuracy of the experiment arrangements.

The effect of the weakening-hole dimensions, their number and position on the shell surface, was evaluated by the following dimensionless parameters: coefficients of reduction of the critical load for weakened shells, $\eta_k = P_k/P_0$ and $\eta_c = P_c/P_0$; coefficients indicating the effect of the weakening-hole radius and of the height of the bridge between the weakening holes, respectively $\omega = \rho^2/R_{av}\delta$ and $c = h/\rho$. Graphs were plotted from the test results, each point representing the average value for three specimens.

Presented in Fig. 7 is the variation of the critical forces with parameter ω, for shells weakened by holes located at midheight and on one side only. It will be seen that the critical forces diminish as ω is increased; also, the greatest reduction rate of η_k (full lines) and η_c (dashed lines) occur in the interval $\omega = 1$ to 10. Concurrently, as ω increases, so the gap between the upper and lower critical-load values is increased. These relationships also apply to shells with different geometric parameters, as is demonstrated in Fig. 8, which shows the scatter envelope of experimental P_k values for shells of length 3D and different D and δ values. For a fairly wide range of geometric parameters of shells with approximately equal weakening parameters ω, the scatter of P_k values amounted to nearly 8%. The same relationship applies also to P_c.

The variation of the critical-load coefficient η_k with the form of the weakening, hole dimension, and shell height, is shown in Fig. 9. For shell lengths of $L \leq 2D$ (shells with $L = 1.5D$ and $L = 2.5D$ were also tested, the data for which are not shown in the figure), the critical loads for both alternative types of weakening can be regarded as identical, as for $\omega = 6$ the divergence was nearly 5%. For shells with $L > 2D$ and the same value of parameter ω, the divergence was about 10%.

Presented in Fig. 10 is the variation of the critical-load coefficient η_c for the same shells. It should be noted that the disparity between the η_c values for different types of weakening is practically constant over the whole range of ω values examined, and amounts to less than 2%; therefore, the value of η_c can be regarded as being the same for a constant value of ω, for both a through-type and a single-sided weakening.

For shells with two holes located on a generatrix, the critical-load coefficients η_k depend on the size of the bridge between the holes (Fig. 11); for shells with different values of the weakening parameter ω it depends on the dimensionless parameter c (Fig. 12).

CONCLUSIONS

1. All cylindrical shells can be divided into two groups according to the dimensions of the weakening holes. The first group comprises shells with parameter $\omega \leq 1.0$, where the weakening effect can be ignored and the loss of stability is of a general nature. Shells in the second group have $\omega > 1$, which characteristically manifest a local loss of stability.

2. For shells with $L \leq 2D$, the critical loads P_k are practically identical for single-sided and through holes. The doubling of the area of sectional weakening in the case of through holes, i. e. when the condition of symmetrical loading of sections is observed, is equivalent, for this type of shell, to a single-sided weakening, i. e., where loading is unsymmetrical. For shells with $L > 2D$ the magnitude of the area of sectional weakening for through holes has a greater effect than the asymmetry of loading, and reduces the values of P_k.

3. The magnitude of the critical load P_k does not depend on the form of weakening (single-sided or through holes), but depends only on the coefficient of stress concentration at the hole boundary.

4. Interaction of weakening holes which are located on the generatrix occurs only in shells with $c = h/\rho < 4$. For $c = 4$, coefficient η_k has the same value as for shells with one hole (if the weakening coefficients ω are identical); and for $c > 4$ an insignificant increase in η_k (up to 4%) is observed, compared with its values for shells with one hole.

5. Shells with through holes, and also with two or more holes on the generatrix (for $c \geq 4$), can be regarded as shells having one hole, provided that their proportions meet the limit $L \leq 2D$.

LITERATURE CITED

1. A. S. Vol'mir, N. L. Vorob'eva, and I. N. Preobrazhenskaya, Review of Investigations of Stability of Plates and Shells [in Russian], in: Design of Space Structures, Izd. Gosstroiizdat, Moscow (1972), 15th ed.
2. V. S. Gavrish, A. P. Shapovalov, et al., "Investigations of post-elastic stability of cylindrical shells with circular perforations," Prikl. Mekhanika, 7, No. 11 (1971).
3. V. S. Gavrish, A. P. Shapovalov, et al., "Clamp for tensile testing of very thin tube specimens in machines type GSM-50, GRM-1 and GRM-2," Zavod. Lab., 38, No. 3 (1972).
4. A. S. Vol'mir, Stability of Systems Subjected to Deformation [in Russian], Izd. Nauka, Moscow (1967).
5. A. N. Guz', Formulation of Stability Problem of Plates and Shells Weakened by Holes [in Russian], in: Stress Concentration, Izd. Naukova Dumka, Kiev (1970), 3rd ed.